

Structural Elucidation of the Lignins from Stems and Foliage of *Arundo donax* Linn.

Ting-Ting You, Jian-Zhen Mao, Tong-Qi Yuan, Jia-Long Wen, and Feng Xu*

Beijing Key Laboratory of Lignocellulosic Chemistry, Beijing Forestry University, Beijing, China

S Supporting Information

ABSTRACT: As one of the potential energy crops, *Arundo donax* Linn. is a renewable source for the production of biofuels and bioproducts. In the present study, milled wood lignin (MWL) and alkaline lignin (AL) from stems and foliage of *A. donax* were isolated and characterized by FT-IR spectroscopy, UV spectroscopy, GPC, ³¹P NMR, 2D HSQC NMR, and DFRC. The results indicated that both stem and foliage lignins were HGS type lignins. The semiquantitative HSQC spectra analysis demonstrated a predominance of β -O-4' aryl ether linkages (71–82%), followed by β - β' , β -5', β -1', and α,β -diaryl ethers linkages in the lignins. Compared to stem lignins, foliage lignins had less β -O-4' alkyl-aryl ethers, lower weight-average molecular weight, less phenolic OH, more H units, and lower S/G ratio. Moreover, tricin was found to incorporate into the foliage lignins (higher content of condensed G units) in significant amounts and might be alkaline-stable.

KEYWORDS: *A. donax*, stem, foliage, lignin, tricin, HSQC, DFRC

INTRODUCTION

Aiming to reduce greenhouse gas emissions and the dependence on fossil fuels, it appears especially crucial to look for new alternative sources of energy. *Arundo donax* is a fast-growing perennial grass with high biomass production, native to East Asia, and widespread throughout the Mediterranean area for thousands of years and has been present in the United States for more than a century.¹ Considered as one of the most promising biomass energy crops in southern Europe, *A. donax* has attracted increasing research for the past decades.

Previous works have dealt with the cultivation, productivity, pyrolysis characteristics, and chemical components of *A. donax*.^{2–8} This species is fast-growing with a growth rate of 0.7 m per week or 10 cm per day under optimum conditions and a high production yield without irrigation supply.^{3,4} The polysaccharides have structural features similar to those isolated from other Gramineae plants.⁶ In addition, their extractive contents are relatively higher than those of other monocotyledons and mainly consist of series of long-chain fatty acids, alkanes, aldehydes, alcohols, monoglycerides, free and esterified sterols and triterpenols, steryl glucosides, steroid hydrocarbons, and steroid and triterpenoid ketones in stem extractive.^{7,8} Moreover, the chemical components of *A. donax* varied among maturity stages and morphological regions (internodes, nodes, root, and foliage).⁹ Potential industrial utilizations of *A. donax* include the use as a source of fiber for paper and chemical feedstocks for the production of bioethanol and other energy products.^{8,10} Most research has focused on investigating nodes and internodes from *A. donax* stems.^{7,8} To achieve the maximum economic value of the whole organism, studies should be focused not only on stems but also on foliage. As lignin plays a key role in pulping and other chemical conversion process, it is necessary to broaden the knowledge of structural features of lignin. However, a comprehensive study of the chemical and structural analysis of *A. donax* lignin is quite scarce and dispersed, especially from the whole stems and the foliage.

Lignin is a complex amorphous polymer and synthesized mainly from three aromatic alcohols (monolignols), namely, *p*-coumaryl, coniferyl, and sinapyl alcohols. During the lignification, each of these monolignols gives rise to a different type of lignin unit called *p*-hydroxyphenyl (H), guaiacyl (G), and syringyl (S) units, respectively.^{11,12} This biosynthesis process consists of mainly radical coupling and creates a unique lignin polymer in each plant species, even in different tissues of the same individual. Most importantly, studies have been reported that these lignin-related phenylpropanoids are precursors not only of lignin but also of anthocyanins, phytoalexins, and flavonoids.¹³

Although the structures of lignin have been studied for more than a century, they have not yet been completely elucidated.^{12,13} A main obstacle in elucidating the structure of lignin is their isolation from lignocellulosic materials in a chemically unaltered form.¹⁴ Milled wood lignin (MWL) proposed by Björkman in 1954 has been used as a representative source of native lignin.¹⁵ However, the yield is not very high even with prolonged ball-milling time.¹⁶ To improve the yield while minimizing the extent of chemical modification of lignin, some other procedures have been developed, such as pretreatment with cellulolytic enzymes, using the combination of enzymatic and mild acidolysis, and completely dissolving in a solvent system followed by precipitation in dioxane/water.^{17–19} In addition, alkaline extraction of lignin (AL) under mild condition is believed to not cause much chemical modification except for saponification of esterified hydroxycinnamic acids, which is particularly suitable for Gramineae plant lignins.²⁰

In the present work, a more in-depth and complete characterization of MWL and AL in stems and foliage of *A. donax* has been performed by the use of an array of analytical

Received: January 9, 2013

Revised: May 5, 2013

Accepted: May 6, 2013

Published: May 6, 2013

techniques, including ultraviolet (UV) spectroscopy, Fourier transform infrared (FT-IR) spectroscopy, gel permeation chromatography (GPC), ^{31}P nuclear magnetic resonance (^{31}P -NMR) spectra, solution state two-dimensional heteronuclear single-quantum coherence NMR (2D HSQC NMR), and derivatization followed by reductive cleavage (DFRC). Among them, 2D HSQC NMR is a powerful tool for lignin structural characterization, revealing both the aromatic units and the different interunit linkages present in the lignin polymer, and provides information on the structure of the whole macromolecule;^{21,22} as a destructive method, DFRC degradation selectively cleaved α - and β -aryl ether bonds, allowing the analysis of the monomeric degradation products released from noncondensed etherified lignin units.²³ Knowledge of the composition and structure of lignin will help to maximize the exploitation of this interesting crop for biomaterial and biofuels production.

MATERIALS AND METHODS

Materials. *A. donax*, 3 years old, was harvested from an experimental field of the Beijing Academy of Agricultural Sciences (China) in May 2009, with an average height of 3.3 m. The stems were separated from foliage. After drying at 55 °C for 16 h in an oven, the stems and foliage were smashed in an FZ120 plant shredder (Truelab, Shanghai, China), sieved to 40–60 mesh. Then the samples were washed by distilled water and extracted with toluene/ethanol (2:1, v/v) in a Blst-250SQ Soxhlet apparatus (Bilon, Shanghai, China) for 6 h and air-dried for 24 h. The extractive-free samples (50 g) were finely ball-milled by a Pulverisette 6 planetary ball mill (Fritsch, Idar-Oberstein, Germany). The milling process was conducted at room temperature for 5 h at 450 rpm with 10 min of rest every 10 min of working. All chemicals used were purchased from Sigma Chemical Co. (Beijing, China) and used as supplied.

Isolation of MWL and AL. The *A. donax* MWLs were obtained and purified from the extractive-free ball-milled plant powder according to the modified Björkman method.²⁴ After extraction of the MWL, the dioxane–water extracted residues were air-dried and treated with 8% aqueous NaOH at 45 °C for 5 h with a solid to liquid ratio of 1:20 (g/mL). The extracting solutions were acidified to pH 5.5–6.0 with 6 M HCl and then concentrated under reduced pressure at 45 °C. The concentrated solution was poured into 3 volumes of 70% ethanol to induce hemicellulosic precipitation. After removal of the hemicelluloses, the lignins in solution were obtained by precipitation at pH 1.5 to 2.0. Finally, the lignin precipitates were washed with acidified water (pH 2.0) and diethyl ether and then freeze-dried overnight.

Chemical Composition. The chemical compositions of the extractive-free *A. donax* were analyzed by using the methods of Laboratory Analytical Procedure (LAP) of biomass provided by the National Renewable Energy Laboratory (NREL).²⁵ The samples were hydrolyzed with 72% sulfuric acid during 1 h at 30 °C in a water bath. After dilution, hydrolysis was performed in a Yxq-Ls-50SII autoclave safe rack (Yuntai, Shanghai, China) for 1 h at 121 °C. Then the hydrolysate was centrifuged for 10 min at 3800 rpm after cooling. Acid-insoluble lignin was determined after filtration and hot water washing over a G4 glass filter crucible. The supernatant fluid was diluted twice to bring the absorbance into the range of 0.7–1.0 and determined the acid-soluble lignin at 320 nm on a UV2300 spectrophotometer (Techcomp, Shanghai, China). The samples for structural carbohydrates were analyzed by high-performance anion chromatography on an ICS3000 instrument (Dionex, Sunnyvale, CA, USA). The column used was a 150 mm \times 3 mm i.d., 4 μm , CarboPac PA20, with a 3 mm \times 30 mm i.d. guard column of the same material (Dionex). The associated hemicelluloses in lignin fractions were also determined by acid hydrolysis and then analyzed by the HPAEC system mentioned above. The indeterminacy of parallel results for carbohydrate analysis was <3%.

UV Spectroscopy. The lignin fractions were dissolved in DMSO and scanned from 500 to 190 nm on a UV 2300 spectrophotometer (Techcomp, Shanghai, China). For comparison, each absorbance

spectrum was plotted as the molar absorptivity by normalizing the UV absorbance to wavelength.

FT-IR Spectroscopy. FT-IR spectra of the isolated lignins were collected in the transmission mode on a Tensor 27 FT-IR spectrophotometer (Bruker AXS, Karlsruhe, Germany), using a KBr disk containing 1% ground samples in the range of 4000–400 cm^{-1} . Thirty-two scans were taken for each sample, and the distinguishability was 4 cm^{-1} .

GPC. The molecular weights of the lignins were performed by Agilent1200 gel permeation chromatography (Agilent, Santa Clara, CA, USA) with a refraction index detector (RID). The column used was a 300 mm \times 7.5 mm i.d., 10 μm , PL-gel Mixed-B, with a 50 mm \times 7.5 mm i.d. guard column of the same material (Agilent, UK). Before the analysis, lignin samples were acetylated with acetyl bromide according to previous literature.²⁶ Then the samples were dissolved in THF (HPLC grade) with a concentration of 1 mg/mL, and 5 μL of solution was injected. The column was operated at 30 °C and eluted with THF at a flow rate of 1 mL/min. The column was calibrated using polystyrene standards.

NMR Spectroscopy. NMR spectra were recorded on a Bruker AVIII 400 MHz spectrometer (Germany) instrument at 25 °C. For ^{31}P NMR experiments, they were conducted according to a previous paper²⁷ with minor modification. Twenty milligrams of lignin was dissolved in 500 μL of anhydrous pyridine and deuterated chloroform (1.6:1, v/v) under stirring. Then 100 μL of cyclohexanol (10.85 mg/mL) was added as an internal standard followed by adding 100 μL of chromium(III) acetylacetonate solution (5 mg/mL in anhydrous pyridine and deuterated chloroform 1.6:1, v/v) as relaxation reagent. Finally, the mixture was reacted with 100 μL of 2-chloro-1,3,2-dioxaphospholane (phosphitylating reagent) for about 10 min. All chemicals used were purchased from Sigma-Aldrich GmbH (Munich, Germany).

For HSQC experiments, the preparation of 80 mg of lignin was carried out using 0.5 mL of DMSO- d_6 . The HSQC experiments used a pulse program with spectral widths of 5000 and 20000 Hz for the ^1H and ^{13}C dimensions, respectively. The number of collected complex points was 1024 for the ^1H dimension with a recycle delay of 1.5 s. The number of transients was 128, and 256 time increments were always recorded in the ^{13}C dimension. $^1J_{\text{CH}}$ used was 145 Hz. Processing used typical matched Gaussian apodization in ^1H and a squared cosine-bell in ^{13}C . The J -coupling evolution delay was set to 3.2 ms. Squared cosine-bell apodization function was applied in both dimensions. Prior to Fourier transformation, the data matrices were zero filled to 1024 points in the ^{13}C dimension. The central solvent (DMSO- d_6) peak was used as an internal reference ($\delta_{\text{C}}/\delta_{\text{H}}$ 39.5/2.49). A semiquantitative analysis of the intensities of the HSQC cross-peak was performed using Bruker Topspin-NMR processing software.

DFRC Degradation. For further characterization, the DFRC degradation was performed according to the protocol developed by Lu and Ralph.²³ The acetylated lignin degradation products were collected after rotary evaporation of the solvents and subsequently analyzed by GC-MS using relative retention times and GC response factors to authenticate the DFRC degraded products. The GC-MS analyses were performed with an Agilent 7890A/5975C instrument (Agilent, Santa Clara, CA, USA). GC-FID and GC-MS used the same 30 m \times 0.25 mm (0.25 μm film thickness) HP-5MS column with He as carrier gas. Chromatography conditions were as follows: initial column temperature, 160 °C, hold for 1 min; ramping at 10 °C/min to 310 °C, hold for 5 min; injector temperature, 250 °C; FID detector temperature, 300 °C; mass spectrometric measurements were performed using electron impact ionization (EI) at 70 eV and a scan range of m/z 50–500; injection volume, 1 μL . Quantitative analysis of the released monomers was performed using tetracosane as internal standard. GC response factors of each individual compound were 1.2, 1.3, and 1.6 for G, P, and S, respectively. The GC response factors for the acylated moieties, 4-acetoxy-3-methoxycinnamyl 4-acetoxyphenylpropionate (G_{pc}) and 4-acetoxy-3,5-dimethoxycinnamyl 4-acetoxyphenylpropionate (S_{pc}), were 2.60 and 3.12, respectively.

RESULTS AND DISCUSSION

Chemical Composition. The relative abundances of the main constituents of *A. donax* are summarized in Table 1. As

Table 1. Abundance of the Main Constituents of Stems and Foliage from *A. donax* (Percent Dry Weight)

main constituent	stems	foliage
toluene/ethanol (2:1, v/v) extractives	10.70	6.50
lignin	19.66	12.45
acid insoluble lignin ^a	18.42	10.13
acid soluble lignin	1.24	2.32
holocellulose	72.60	44.71
cellulose	42.15	24.35
hemicelluloses	30.45	20.36
arabinan	1.52	2.65
galactan	0.45	0.77
xylan	28.48	16.94
mannan	tr ^b	tr
ash	2.98	12.93
total mass	95.24	70.09

^aThe acid insoluble lignin was corrected by ash. ^bTrace.

can be seen, the stems had higher holocellulose and lignin contents (72.6 and 19.7%, respectively) and lower ash content (2.98%) compared with foliage and other common gramineous plants, such as wheat straw and elephant grass.^{28,29} These agreed well with the data reported in a previous paper.⁹ The stems presented an acid-insoluble lignin content of 18.4% (based on the oven-dried stems) that amounted up to 19.6% by taking into account the acid-soluble lignin (1.2%), which was higher than observed in foliage (12.5%), mainly resulting from the higher level of lignification. The content of hemicelluloses was different in each fraction of the *A. donax*. The higher xylose contents (16.9–28.5%) of stems make them very attractive for the use of *A. donax* as a source of pentosans for the furfural-based industry. There was no significant difference in arabinan and galactan between stems and foliage. However, the ash content in the foliage was approximately 6 times higher than

that in the stems, which was also reflected in the higher amount of inorganic elements. Compared with the foliage, the extractive content of the stems was higher (10.7%); this was reflected in elevated levels of aromatics, sterols, alkane, fatty acids, and alcohol in the stems than in the foliage, which was inconsistent with some other herbaceous plants.³⁰

Yield and Sugar Analysis. The extensive use of rotary ball milling (dry) resulted in the depolymerizing structure of lignin macromolecule, increasing the content of phenolic β -O-4' and α -O-4', even causing some condensation reaction. To minimize the damage of structure change arising by ball-milling, the extractive-free materials were ball-milled for only 5 h. In the first step, MWL was extracted from the ball-milled materials; in the subsequent stage, 8% aqueous NaOH was used to obtain

Table 2. Neutral Sugar and Uronic Acid Contents (Percent, \pm 3%)^a of the Isolated Lignin Fractions

sugar	lignin fractions			
	stem MWL	foliage MWL	stem AL	foliage AL
arabinose	0.17	0.28	nd ^b	0.22
galactose	nd	0.54	nd	0.20
glucose	0.40	6.18	0.07	1.79
xylose	10.67	4.81	0.06	4.33
mamnose	0.13	nd	nd	nd
uronic acid	0.50	nd	nd	nd
total carbohydrate	11.87	11.81	0.13	6.53
yield	5.41	4.42	9.82	5.6

^aPooled standard error. ^bNot detected.

Table 3. Results of Weight-Average (M_w) and Number-Average (M_n) Molecular Weights and Polydispersity Indices (M_w/M_n) of Lignin Preparations

	lignin fractions			
	stem MWL	foliage MWL	stem AL	foliage AL
M_w	2460	2060	1370	1350
M_n	1260	1080	950	910
M_w/M_n	1.95	1.91	1.44	1.48

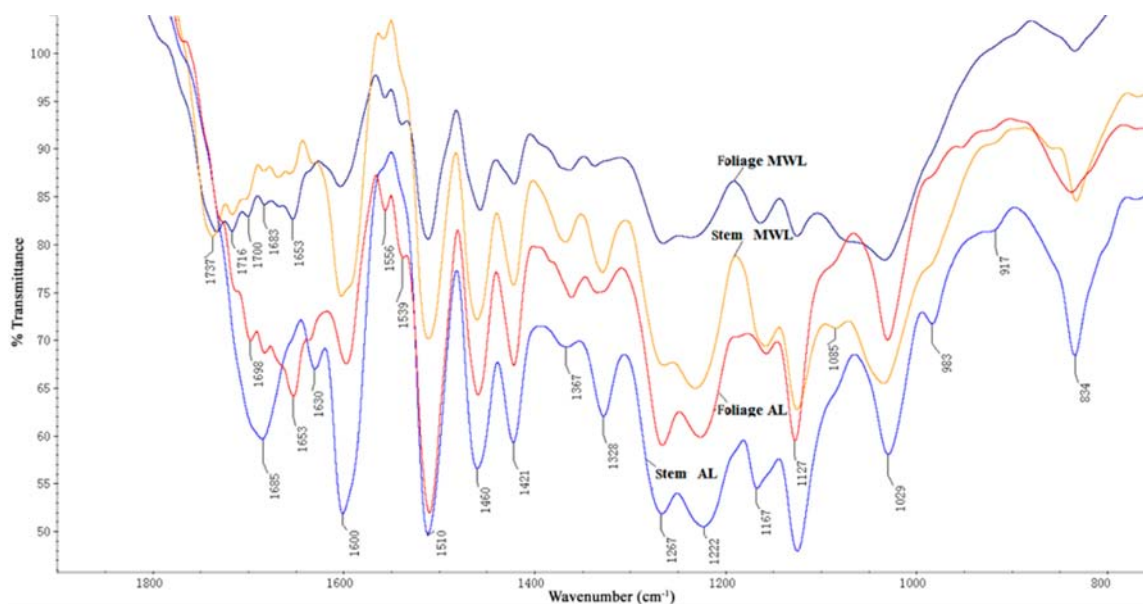


Figure 1. FT-IR spectra of stem MWL, foliage MWL, stem AL, and foliage AL.

more representative lignin samples for structural characterization, which was demonstrated to saponify main ester bonds between hemicelluloses and lignin.²⁰ Table 2 shows the yield and sugar content of each fraction. As expected, the low yield of MWLs (ranging from 4.42 to 5.41% of the original total lignin) might be related to the low severity for milling and multistep purification processes, which were in accordance with the previous literature.³¹ Furthermore, the yield of ALs ranging from 5.60 to 9.82% of the original total lignin.

Lignin is difficult to isolate purely and completely from gramineous plants on account of the linkages associating with cell wall carbohydrate polymers, such as forming ferulic acid bridge via ester linkage with arabinoxylans.³² Sugar analysis indicated that both stems and foliage MWL contained relatively noticeable amounts of associated carbohydrates (11.87 and 11.81%, respectively), whereas the contents of the carbohydrates in stem AL and foliage AL were <7%. This phenomenon might be explained by the cleavage of ester linkages between lignin and carbohydrates. Xylose, glucose, and arabinose were observed as the major sugars in the four fractions, whereas mannose and uronic acid appeared in trace amount. A small amount of galactose was also detected in foliage (0.54% in MWL, 0.20% in AL), but it was difficult to find in stems.

Molecular Weight Distributions. The values of the weight-average (M_w) and number-average (M_n) molecular weights, estimated from GPC curves (relative values related to polystyrene standard) and polydispersity indices (M_w/M_n , PI) of the MWL and AL isolated from *A. donax* stems and foliage are presented. As illustrated in Table 3, the M_w values of lignins from stems (2460 g/mol in MWL, 1370 g/mol in AL) were apparently higher than those from foliage (2060 g/mol in MWL, 1350 g/mol in AL). This phenomenon may be due to the different lignification levels between stems and foliage. Additionally, the M_w of ALs from stems and foliage were lower than the corresponding MWLs. One reason for that might be related to the higher contents of carbohydrates associated with the MWLs.³³ On the other hand, the ester linkages between hydroxycinnamic acid and lignin might be cleaved partly by 8% aqueous NaOH, leading to a significant degradation of the lignin macromolecules.³² Moreover, all of the lignins exhibited relatively narrow molecular weight distribution (PI < 2.0), and MWLs showed a relatively higher PI as compared to the corresponding ALs.^{31,32}

UV Analysis. All four lignins showed similar UV spectra, exhibiting two absorption maxima around 280 and 310 nm. The former absorption maximum probably originated from the free and etherified hydroxyl group in aromatic rings, and the latter one was due to bound hydroxycinnamic acid in gramineous plants, especially a predominance of esterified *p*-coumaric acid.^{32,34} It is well-known that the absorbance coefficient of UV spectra demonstrates the purity of lignins.³⁵ Compared to the MWLs, the higher absorbance coefficient of ALs indicated that lignin with higher purity could be obtained when aqueous alkaline was used as a solvent. A slightly lower absorbance coefficient in foliage lignins suggested that the foliage lignins contained more nonlignin materials than in stems. This was in line with the results of sugar analysis as shown in Table 2.

FT-IR Analysis. The FT-IR spectra of the four lignin fractions are illustrated in Figure 1. As can be seen from the spectra, the four lignins showed similar spectroscopic patterns, indicating the similar structures are present in the lignins. The aromatic skeleton vibrations in lignin are assigned at 1605, 1510, and 1420 cm^{-1} . Absorbance for these bands appearing at

Table 4. Lignin Structural Characteristics from Integration of ^{13}C – ^1H Correlation Signals in the HSQC Spectra, ^{31}P NMR Spectra, and DFRC Results of the MWLs and ALs of Stems and Foliage from *A. donax*

characteristic	lignin fractions			
	stem MWL	foliage MWL	stem AL	foliage AL
linkages (% C_9 units)				
β -O-4' aryl ether (A, A', A'')	79	71	82	71
resinol (B)	9	10	5	8
phenylcoumaran (C)	8	12	6	10
spirodienone (D)	3	6	4	2
α,β -diaryl ethers (E)	1	1	3	9
acylation degree (major γ -acylation)	43	60	5	7
lignin aromatic units ^a (%)				
H	1	14	1	19
G	61	75	48	43
S	38	11	51	38
<i>p</i> -hydroxycinnamates ^b				
<i>p</i> -coumarates to ferulates ratio	4.9	8.5	2.5	0.5
syringyl to guaiacyl ratio				
S/G (HSQC)	0.62	0.15	1.10	0.88
S/G (DFRC)	0.7	1.07	1.60	1.10
monomers yields from DFRC ^c (% lignins)				
G_{pc} yields from DFRC ^d (%)	6	31	6	6
S_{pc} yields from DFRC ^e (%)	27	78	8	17
aliphatic OH (mmol/g)				
α -OH	2.92	1.88	3.23	1.72
primary OH	1.49	1.01	1.10	0.46
phenolic OH (mmol/g)				
S-OH	1.43	0.87	2.13	1.26
G _{5,5} -OH	0.89	0.69	1.96	0.78
G-OH	0.19	0.22	0.40	0.18
H-OH	0.08	0.06	0.12	0.07
<i>p</i> -coumarates-OH	0.35	0.26	0.74	0.40
COOH (mmol/g)	tr ^f	0.02	T	0.03
	0.27	0.13	0.70	0.10
	0.02	0.01	0.81	0.25

similar intensities revealed that the "core" of the lignin structure did not change significantly during the alkaline treatment. The 1129 cm^{-1} (typical aromatic C–H bending in-plane for S units) and 834 cm^{-1} bands (C–H out-of-plane in positions 2 and 6 of S units and in all positions of H units) showed the features of HGS type lignin. Besides, the absorption band at 1167 cm^{-1} , which is attributed to C=O in ester groups (conjugated), also corroborated that the lignin in both stems and foliage belonged to HGS type.³⁶ Spectra of MWLs showed strong absorbances at 1735 and 1714 cm^{-1} , which are due to C=O stretching in esterified phenolic acids and acetyls. The fact that the bands showed a strong absorbance in MWLs but not in ALs suggested the hydrolysis of ester bonds during the alkaline treatment. The foliage AL showed stronger absorption bands at 1684 cm^{-1} (in the region of α,β -unsaturated carbonyl), indicating that some of

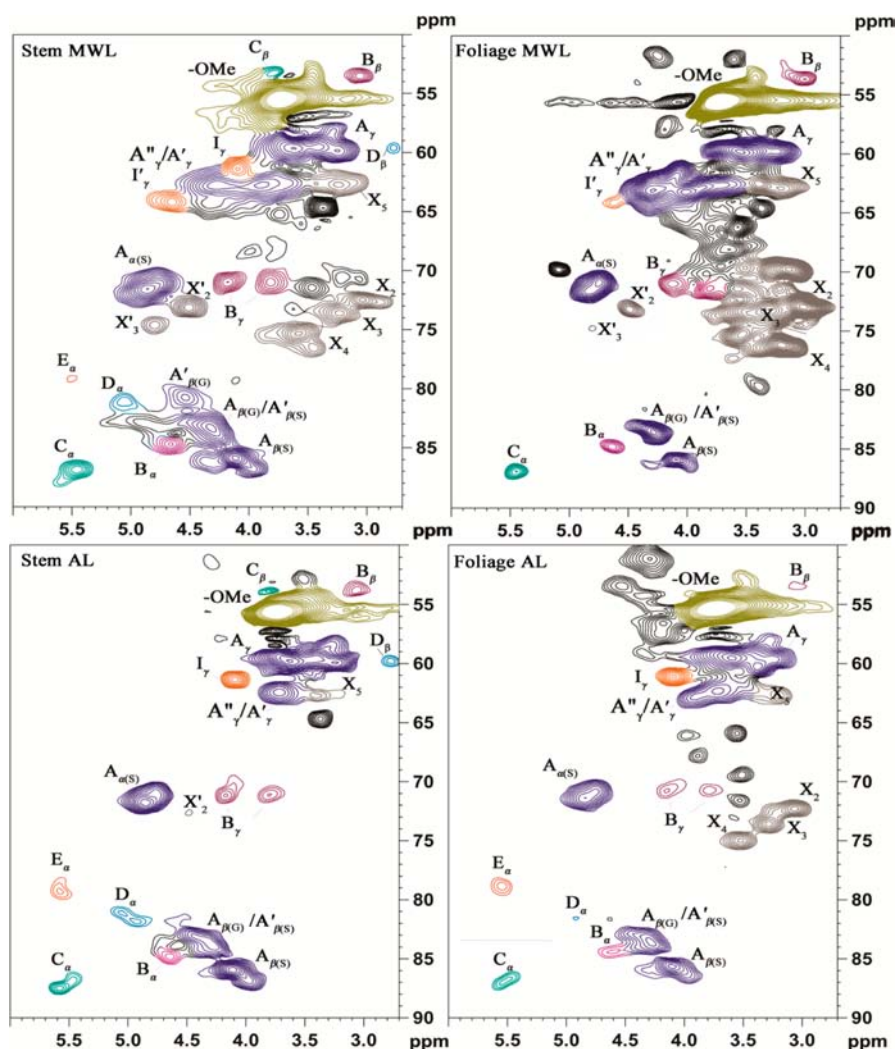


Figure 2. Aliphatic-oxygenated region, δ_C/δ_H 50–90/2.5–6.0, of the HSQC spectra of the lignins from stem MWL, foliage MWL, stem AL, and foliage AL. The main cross-signals of lignin fractions are identified by different colors, whereas carbohydrate signals are presented in gray. See Table 4 for signal assignment and Figure 4 for the main lignin structures identified.

the hydroxyl in foliage lignin changed into unsaturated carbonyl during alkaline treatment.³⁷ MWL and AL of foliage also showed sharp bands at 1653 cm^{-1} , probably arising from the tricinn associated with lignin.³⁸

NMR Analysis. ³¹P NMR Analysis. Application of ³¹P NMR allows qualitative detection and quantitative determination of labile hydroxyl groups (i.e., aliphatic OH, phenolic OH, and carboxylic acids) in lignins. The main lignin signals in the ³¹P NMR spectra were assigned by comparison with the published literature.^{27,39} For aliphatic OH, signals of the α -OH appeared between 136 and 133.8 ppm, whereas signals from primary OH ranged from 133.4 to 132 ppm. For phenolic OH, S-OH, G_{5,5}-OH, G-OH, and *p*-coumarate-OH were distinguished at 132–131.5, 131.5–131, 130.5–129.5, and 128.8–128 ppm, respectively. Additionally, the signals of the COOH group were located in the range of 127.5–126 ppm, and small signals at 129.3–128.8 ppm in foliage lignins may originate from H-hydroxyl groups. The quantitative results of hydroxyl groups were obtained by peak integration with cyclohexanol (signals at 133.8–133.3 ppm) as internal standard and are shown in Table 4.

As can be seen from Table 4, compared with MWLs, the overall amount of primary OH in ALs increased by 0.70 and 0.39 mmol/g in stem AL and foliage AL, respectively, and

the overall amount of COOH group increased by 0.79 and 0.24 mmol/g. These phenomena obviously corresponded to the cleavage of ester bonds in lignins during alkaline treatment, especially the acylated units in the γ -position.⁴⁰ In addition, more primary OH in stem MWL suggested that stem MWL was less acylated than foliage MWL in the γ -position. Moreover, the content of OH in stem AL was the highest among the four lignins.

2D HSQC NMR Analysis. 2D NMR is considered to be a powerful structural elucidation technique and has been widely applied to lignin characterization.^{41,42} To obtain the detailed molecular structures of ALs and MWLs, these lignins were analyzed by solution 2D HSQC NMR. The aliphatic-oxygenated (side chain, δ_C/δ_H 50–90/2.5–6.0) and aromatic (δ_C/δ_H 90–160/6.0–8.0) regions of the spectra of the four lignins are shown in Figures 2 and 3. The main lignin cross-signals in the HSQC spectra were assigned by comparison with the published literature and are listed in Table 5, and the main substructures are depicted in Figure 4.^{22,24,28,29,31,43–45}

The aliphatic-oxygenated region of the spectra (Figure 2) gave useful information about the different interunit linkages presenting in the stems and foliage lignins, such as β -O-4', β -5', β - β' , β -1', etc. In this region, cross-signals of methoxy groups (δ_C/δ_H 55.9/3.73) and side chains in β -O-4' substructures

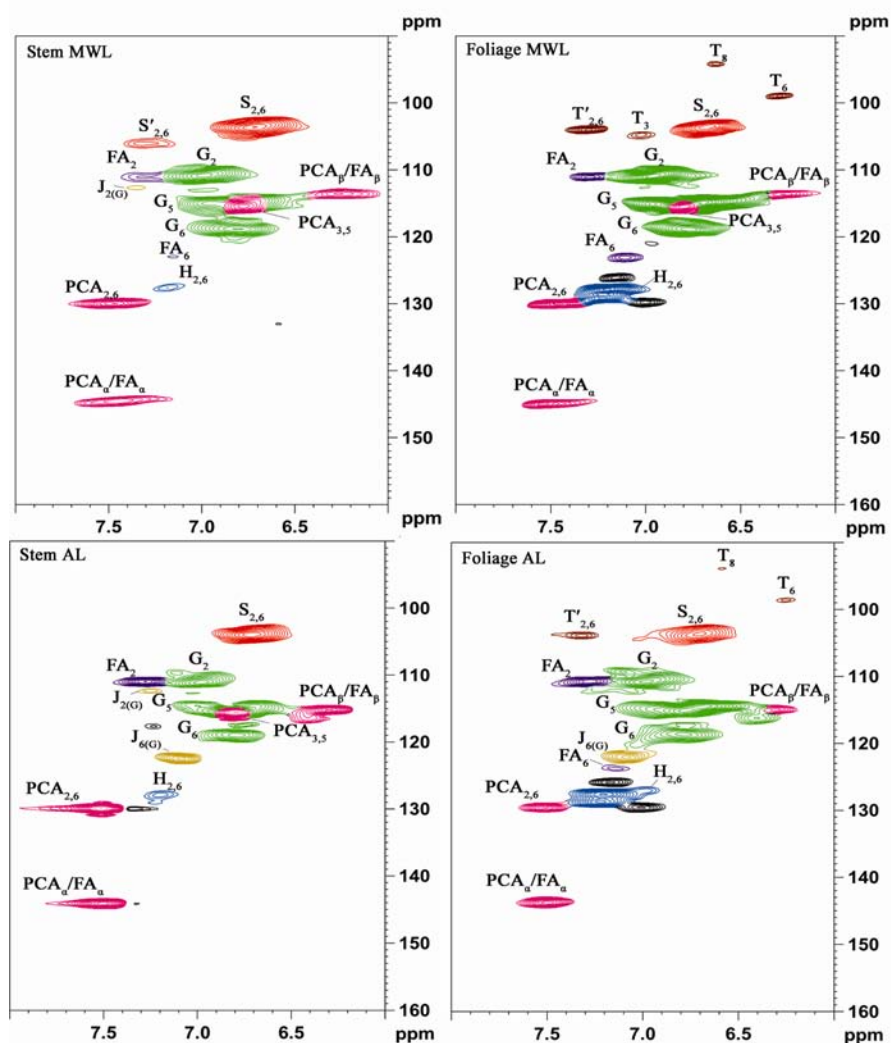


Figure 3. Aromatic region, δ_C/δ_H 90–160/6.0–8.0, of the HSQC spectra of the lignins from stem MWL, foliage MWL, stem AL, and foliage AL. The main cross-signals of lignin fractions are identified by different colors, whereas carbohydrate signals are presented in gray. See Table 4 for signal assignment and Figure 4 for the main lignin structures identified.

(A/A'/A'') were the most predominant. The C_α - H_α correlation in β -O-4' substructure linked to S units ($A_{\alpha(S)}$) was detected at δ_C/δ_H 71.4/4.86, whereas the signal linked to G units ($A_{\alpha(G)}$, δ_C/δ_H 71.0/4.74) was somewhat overlapped. Generally, the C_β - H_β correlations corresponding to β -O-4' substructure linked to S units ($A_{\beta(S)}$) and G units ($A_{\beta(G)}$) are distinguished at δ_C/δ_H 85.9/4.12 and δ_C/δ_H 83.4/4.31, respectively. However, the C_β - H_β correlation of β -O-4' ($A'_{\beta(G)}$) linked to G units shifts from 83.4/4.31 ppm to δ_C/δ_H 81.0/4.49, whereas the C_β - H_β correlation of β -O-4' ($A'_{\beta(S)}$) linked to S units shifts from δ_C/δ_H 85.9/4.12 to δ_C/δ_H 83.4/4.31 as a result of acylation at the γ -carbon position.²⁹ Obviously, the signal at δ_C/δ_H 83.4/4.31 can arise by $A'_{\beta(S)}$ and $A_{\beta(G)}$. The signal of $A'_{\beta(G)}$ was easily found in the HSQC spectra of stem MWL, whereas it was difficult to observe in MWL of the foliage, suggesting a greater acylation extent of G units in stem MWL than foliage MWL. It also clearly showed the presence of intense signals corresponding to acylated γ -carbon in β -O-4' substructure (A'/A'') in the range between δ_C/δ_H 62.7/3.83 and δ_C/δ_H 62.7/4.30. Therefore, the HSQC spectra of *A. donax* demonstrated that the lignin is extensively acylated mainly in the γ -position of the side chain of lignin.

Other linkages among lignin units such as β -5', β - β' , and β -1' were also observed in lower amounts. The signals of C_α - H_α , C_β - H_β , and the double C_γ - H_γ correlations of resinol β - β' substructure (B) were detected at δ_C/δ_H 84.8/4.66, 53.6/3.06, and 71.1/4.19, and 3.82, respectively. However, the signals for a β - β' -linked tetrahydrofuran structure (B') were not detected in the spectra of both MWLs of stems and foliage, although with a high acylation degree (43% in stem MWL and 60% in foliage MWL). These were inconsistent with previous papers, which might be due to different kinds of raw materials.^{29,40,44} The content of phenylcoumaran β -5' substructures (C) was close to resinol (B) in each lignin. The cross peaks at δ_C/δ_H 53.2/3.80 and 86.6/5.47 are attributed to their C_β - H_β and C_α - H_α correlations, respectively. Minor amounts of spirodienone β -1' substructures (D) were detected in stem lignins, but barely detected in foliage lignins. Moreover, α,β -diaryl ether substructures (E) were also observed at δ_C/δ_H 79.2/5.52 with a small amount in these lignins. Other small signals in the side-chain region of the HSQC corresponded to *p*-hydroxycinnamyl alcohol end groups (I), and associated carbohydrates were also observed. The C_γ - H_γ correlations of cinnamyl alcohol end groups (I) were found at δ_C/δ_H 61.3/4.09, whereas the C_γ - H_γ

Table 5. Assignments of Main Lignin ^{13}C – ^1H Correlation Signals^a in the HSQC NMR Spectra Shown in Figures 2 and 3

label	$\delta_{\text{C}}/\delta_{\text{H}}$	assignment	label	$\delta_{\text{C}}/\delta_{\text{H}}$	assignment
Lignin Cross-Peak Signals			Lignin Cross-Peak Signals		
C_{β}	53.2/3.80	C_{β} – H_{β} in phenylcoumaran (β -5') substructures (C)	T_6	98.9/6.28	C_6 – H_6 in triclin (T)
B_{β}	53.6/3.06	C_{β} – H_{β} in resinol (β - β') substructures (B)	$S_{2,6}$	103.7/6.71	$C_{2,6}$ – $H_{2,6}$ in etherified syringyl units (S)
A_{γ}	59.65/3.61 and 3.27	C_{γ} – H_{γ} in β -O-4' substructures (A)	$T'_{2,6}$	103.9/7.30	$C_{2',6'}$ – $H_{2',6'}$ in triclin (T)
D_{β}	59.77/2.78	C_{β} – H_{β} in spirodienone (β -1') substructures (D)	T_3	104.7/7.03	C_3 – H_3 in triclin (T)
I_{γ}	61.3/4.09	C_{γ} – H_{γ} in cinnamyl alcohol end-groups (I)	$S'_{2,6}$	106.7/7.28	$C_{2,6}$ – $H_{2,6}$ in C_{α} -oxidized ($C_{\alpha}=\text{O}$) phenolic syringyl units (S')
A'_{γ}/A''_{γ}	62.7/3.83–4.30	C_{γ} – H_{γ} in γ -acylated β -O-4' substructures (A'/A'')	G_2	110.7/6.98	C_2 – H_2 in guaiacyl units (G)
I'_{γ}	64.0/4.79	C_{γ} – H_{γ} in γ -acylated cinnamyl alcohol end-groups (I')	FA_2	111.0/7.32	C_2 – H_2 in ferulate (FA)
B_{γ}	71.1/3.82 and 4.19	C_{γ} – H_{γ} in resinol (β - β') substructures (B)	$J_{2(G)}$	112.24/7.25	C_2 – H_2 in cinnamyl aldehyde end-groups (J)
$A_{\alpha(S)}$	71.4/4.86	C_{α} – H_{α} in β -O-4' substructures linked to a S unit (erythro) (A)	PCA_{β} and FA_{β}	113.5/6.27	C_{β} – H_{β} in p -coumarate (PCA) and ferulate (FA)
E_{α}	79.2/5.52	C_{α} – H_{α} in α,β -diaryl ether substructures (E)	G_5	114.9/6.72 and 6.94	C_5 – H_5 in guaiacyl units (G)
D_{α}	81.0/5.01	C_{α} – H_{α} in spirodienone (β -1') substructures (D)	$PCA_{3,5}$	115.5/6.77	$C_{3,5}$ – $H_{3,5}$ in p -coumarate (PCA)
$A'_{\beta(G)}$	81.0/4.49	C_{β} – H_{β} in γ -acylated β -O-4' substructures linked to a G unit (A')	G_6	118.7/6.77	C_6 – H_6 in guaiacyl units (G)
$A_{\beta(G)}$ and $A'_{\beta(S)}$	83.4/4.31	C_{β} – H_{β} in β -O-4' substructures linked to a G unit (A) and in γ -acylated β -O-4' substructures linked to a S unit (A')	$J_{6(G)}$	122.3/7.10	C_6 – H_6 in cinnamyl aldehyde end-groups (J)
$D_{\alpha'}$	84.65/4.67	C_{α} – H_{α} in spirodienone (β -1') substructures (D)	FA_6	123.1/7.15	C_6 – H_6 in ferulate (FA)
B_{α}	84.8/4.66	C_{α} – H_{α} in resinol (β - β') substructures (B)	$H_{2,6}$	127.8/7.22	$C_{2,6}$ – $H_{2,6}$ in p -hydroxyphenyl units (H)
$A_{\beta(S)}$	85.9/4.12	C_{β} – H_{β} in β -O-4' substructures linked to a S unit (erythro) (A)	$PCA_{2,6}$	129.9/7.46	$C_{2,6}$ – $H_{2,6}$ in p -coumarate (PCA)
C_{α}	86.6/5.47	C_{α} – H_{α} in phenylcoumaran (β -5') substructures (C)	PCA_{α} and FA_{α}	144.7/7.45	C_{α} – H_{α} in p -coumarate (PCA) and ferulate (FA)
T_8	94.4/6.64	C_8 – H_8 in triclin (T)	Polysaccharide Cross-Peak Signals		
			X_5	63.2/3.26 and 3.95	C_5 – H_5 in β -D-xylopyranoside
			X_2	72.9/3.14	C_2 – H_2 in β -D-xylopyranoside
			X'_2	73.0/4.49	C_2 – H_2 in 2-O-Ac- β -D-xylopyranoside
			X_3	74.1/3.32	C_3 – H_3 in β -D-xylopyranoside
			X'_3	74.7/4.79	C_3 – H_3 in 3-O-Ac- β -D-xylopyranoside
			X_4	75.6/3.63	C_4 – H_4 in β -D-xylopyranoside

^aSignals were assigned by comparison with the literature.^{22,24,28,29,31,43–45}

correlation of cinnamyl alcohol end-groups shifted to $\delta_{\text{C}}/\delta_{\text{H}}$ 64.0/4.79 as a result of γ -acylated I substructure (I'_{γ}).²⁹ It was noted that the side-chain regions of the HSQC spectra of both stems and foliage MWLs showed a strong C_2 – H_2 correlation of 2-O-Ac- β -D-Xylp (X_2') at $\delta_{\text{C}}/\delta_{\text{H}}$ 73.0/4.49 and C_3 – H_3 in 3-O-Ac- β -D-Xylp (X_3' , $\delta_{\text{C}}/\delta_{\text{H}}$ 74.7/4.79), whereas these signals disappeared in alkaline lignins. The stronger signal of X_3' in stem MWL was indicative of the fact that there was more acylated xylan in stem MWL rather than in foliage MWL, which might contribute to the abundance of acetyl groups in MWLs.³⁴

The main cross-signals in the aromatic regions of the HSQC spectra correspond to the aromatic rings of different lignin units and olefinic side chain of hydroxycinnamic acids (Figure 3). Cross-signals from p -hydroxyphenyl (H), syringyl (S), and guaiacyl (G) lignin units could be clearly observed in the spectra of both stem lignins and foliage lignins. The S units showed a prominent signal for the $C_{2,6}$ – $H_{2,6}$ correlation at $\delta_{\text{C}}/\delta_{\text{H}}$ 103.7/6.71. In addition, signals corresponding to $C_{2,6}$ – $H_{2,6}$ correlations in C_{α} -oxidized S units (S' , $\delta_{\text{C}}/\delta_{\text{H}}$ 106.7/7.28) were also present in the spectra with a lower amount only in stem MWL. The G units showed different correlations for C_2 – H_2 , C_5 – H_5 , and C_6 – H_6 at $\delta_{\text{C}}/\delta_{\text{H}}$ 110.7/6.98, 114.9/6.72–6.94, and 118.7/6.77, respectively. Two signals in H units were assigned to $C_{3,5}$ – $H_{3,5}$ and $C_{2,6}$ – $H_{2,6}$ correlations at $\delta_{\text{C}}/\delta_{\text{H}}$ 115.4/6.63 and 127.8/7.22, whereas the former were overlapped with those from the G 5-position. These cross-signals in foliage lignins were more intense than those in stems, indicating a higher content of H units in foliage. However, the aromatic cross-signals of the

cinnamyl alcohol end-groups (I) were overlapped with the same signals in S and G units. Instead, the olefinic correlations of the cinnamyl aldehyde end-groups structures (J) were observed at $\delta_{\text{C}}/\delta_{\text{H}}$ 112.24/7.25 and 122.3/7.10, respectively. These cross-signals were clearly detected in the spectra of the lignins from stems. Furthermore, as were typical in spectra from grasses, prominent signals corresponding to p -coumarate (PCA) and ferulate (FA) structures were also observed. Finally, it was noteworthy that some cross-signals of triclin (T, 5,7,4'-trihydroxy-3',5'-dimethoxyflavone) arose in the HSQC spectra of foliage MWL and AL. The triclin signals corresponded to aromatic C_3 – H_3 ($\delta_{\text{C}}/\delta_{\text{H}}$ 104.7/7.03), C_6 – H_6 ($\delta_{\text{C}}/\delta_{\text{H}}$ 98.9/6.28), C_8 – H_8 ($\delta_{\text{C}}/\delta_{\text{H}}$ 94.4/6.64), and $C_{2',6'}$ – $H_{2',6'}$ ($\delta_{\text{C}}/\delta_{\text{H}}$ 103.9/7.30).^{28,45} As is well-known, triclin is widely distributed in Gramineae plants, including cereal plants of stalks and leaves.⁴⁵ According to the previous papers, the triclin skeleton can be linked to a phenylpropanoid moiety through a β -O-4' bond, which may be incorporated into lignification of plants, acting as lignin monomers.²⁸ The appearance of triclin in foliage MWL of *A. donax* might be good proof of this, and the similar signals in foliage AL suggested that the linkages between triclin and lignin might be alkaline-stable.

The relative abundances of the main lignin interunit linkages and the degree of γ -acylation, as well as the molar abundances of the different lignin units (H, G, and S) and the molar S/G ratios of the lignins in stems and foliage, evaluated from volume integration of contours in the HSQC spectra, are given in Table 4.^{22,46} The semiquantitative HSQC spectra results of

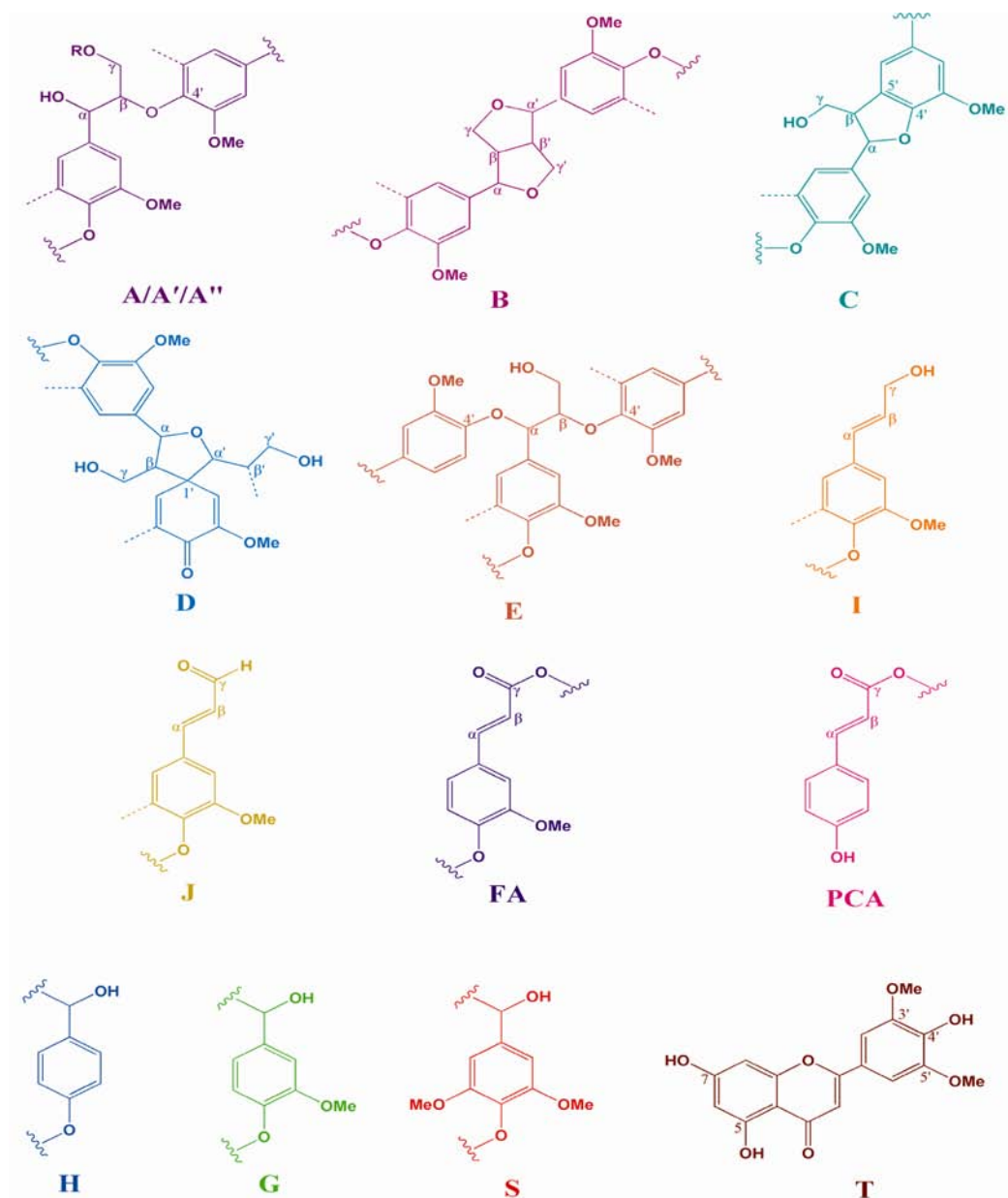


Figure 4. Main structures of lignin fractions of *Arundo donax*, involving different side-chain linkages, and aromatic units identified by 2D HSQC NMR: (A) β -O-4' linkages; (A') β -O-4' linkages with acetylated γ -carbon; (A'') β -O-4' linkages with *p*-coumaroylated γ -carbon; (B) resinol structures formed by β - β' , α -O- γ' , and γ -O- α' linkages; (C) phenylcoumarane structures formed by β -5' and α -O-4' linkages; (D) spirodienone structures formed by β -1' and α -O- α' linkages; (E) α , β -diaryl ether substructures; (H) *p*-hydroxyphenyl unit; (G) guaiacyl unit; (S) syringyl unit; (I) cinnamyl alcohol end-groups; (J) cinnamyl aldehyde end-groups; (FA) ferulate; (PCA) *p*-coumarate; (T) triclin.

these lignins demonstrated a predominance of β -O-4' aryl ether linkages (71–82%), followed by the similar amounts of β - β' resinols and β -5' phenylcoumaran in each lignin. The content of β -O-4' aryl ether linkages was much higher than in flax (50–58%).²⁴ Moreover, a minor amount of β -1' spirodienone (2%–6%) was also observed. The α , β -diaryl ethers in stem MWL and foliage MWL were very small, but increasing in ALs in both stems and foliage. With respect to acylation, the MWLs were extensively acylated (43–60%) at the γ -carbon of the side chain. In contrast, the acylation degrees of ALs were much lower (5–7%). Moreover, the *p*-coumarates to ferulates ratio in foliage MWL (8.5) was higher than that in stem MWL (4.9), and the ratios decreased in both stem AL (2.5) and foliage AL (0.5). Compared to foliage MWL, stem MWL had less H unit content and higher S/G ratio (0.15–0.62). It had

been reported that triclin in wheat straw lignin was etherified by G units.²⁸ The appearance of triclin in foliage with higher G unit content might be good evidence for this.

DFRC Degradation Analysis. To figure out the syringyl to guaiacyl ratio in lignins of noncondensed structures, the MWLs and ALs were degraded by DFRC method. The lignins released acetylated derivatives of *cis*- and *trans*-isomers of syringyl (S_c and S_t) lignin, guaiacyl (G_c and G_t), *p*-hydroxyphenyl (P_c and P_t), and G_{pc} and S_{pc} monomers.^{29,47} As expected, the results of integration of areas showed a remarkable amount of *trans*-isomers in MWLs of stems and foliage.⁴⁸ The *trans*-isomers of S, G, and H decreased after alkaline treatment, as the stereochemical structures of lignins might change during the process. The DFRC quantitative analysis indicated that the yield of the main monomers (G, S, P, G_{pc} and S_{pc}) of stem MWL recovered

from DFRC degradation was relatively lower than the others, which might reflect a higher content of α -carbonyl groups in the side chain of stem MWL according to previous literature.⁴⁹ The S/G ratios of stem lignins evaluated by the DFRC method ($S/G_{(DFRC)}$) were close to the data obtained via 2D-NMR ($S/G_{(HSQC)}$), whereas the $S/G_{(DFRC)}$ ratios (0.15 and 0.88 in MWL and AL, respectively) of foliage lignins were somewhat different from $S/G_{(HSQC)}$ ratios (1.11 and 1.13 in MWL and AL, respectively). This demonstrated a higher content of condensed G units in foliage lignins than in stem lignins, which might be partly related to the etherified linkages between triclin and G units.²⁸ As shown in Table 4, a large amount of the *p*-coumaroylated units were detected in the γ -position of these lignins, especially on the syringyl units, which was in line with a previous study.²⁹ After alkaline treatment, the *p*-coumaroylated units decreased due to the cleavage of ester bonds between the *p*-coumarate and lignins.

In summary, the analysis of the MWLs from of *A. donax* indicated that both stems and foliage MWLs were HGS type lignins, and the S/G ratio was 0.15–0.62, with a strong predominance of G units. The hydroxycinnamic acid was primary *p*-coumaric acid, which attached to lignin via ester bonds, which were cleaved during alkaline treatment (AL). The main lignin interunit linkages are β -O-4' alkyl-aryl ethers, followed by β - β' , β -5', β -1', and α,β -diaryl ethers, together with cinnamyl alcohol and cinnamaldehyde end-groups. However, the tetrahydrofuran structure was not detected in the HSQC spectra of both MWLs of stems and foliage even with high acylation degrees. Some structural differences between stems and foliage lignins were also observed. Compared to stem lignins, foliage lignins had fewer β -O-4' alkyl-aryl ethers, lower weight-average molecular weight, less phenolic OH content, more H units, higher condensed G units, and lower S/G ratio. Additionally, the foliage lignin with higher condensed G units contained a greater amount of triclin, and the linkage between lignin and triclin might be alkaline-stable. The comprehensive structural elucidation of lignins in the whole stems and foliage of *A. donax* will provide a theoretical basis for further use in pulping, biomaterials, biofuels, and green chemical production.

■ ASSOCIATED CONTENT

Supporting Information

Additional figures and table. This material is available free of charge via the Internet at <http://pubs.acs.org>.

■ AUTHOR INFORMATION

Corresponding Author

*Phone: +86-10-62336387. Fax: +86-10-62336903. E-mail: xfx315@bjfu.edu.cn.

Funding

We gratefully acknowledge financial support from the National Natural Science Foundation of China (31225005 and 31070526), the National Science and Technology Program of the Twelfth Five-Year Plan Period (2012BAD32B06), and the Natural Science Foundation of Heilongjiang Province for distinguished young scholars (JC200907).

Notes

The authors declare no competing financial interest.

■ REFERENCES

(1) Sarkhota, D. V.; Grunwalda, S.; Geb, Y.; Morgan, C. L. S. Total and available soil carbon fractions under the perennial grass *Cynodon*

dactylon (L.) Pers and the bioenergy crop *Arundo donax* L. *Biomass Bioenerg.* **2012**, *41*, 122–130.

(2) Nassi, N.; Angelini, L. G.; Bonari, E. Influence of fertilisation and harvest time on fuel quality of giant reed (*Arundo donax* L.) in central Italy. *Eur. J. Agronom.* **2010**, *32*, 219–227.

(3) Bell, G. P. Ecology and management of *Arundo donax*, and approaches to riparian habitat restoration in southern California. In *Book Plant Invasions: Studies from North America and Europe*; Brock, J. H., Wade, M., Pysek, P., Green, D., Eds.; Blackhuys Publishers: Leiden, The Netherlands, 1997; pp 103–113.

(4) Mantineo, M.; D'Agosta, G. M.; Copani, V.; Patanè, C.; Cosentino, S. L. Biomass yield and energy balance of three perennial crops for energy use in the semi-arid Mediterranean environment. *Field Crop Res.* **2009**, *114*, 204–213.

(5) Jeguirim, M.; Dorge, S.; Trouvé, G. Thermogravimetric analysis and emission characteristics of two energy crops in air atmosphere: *Arundo donax* and *Miscanthus giganteus*. *Bioresour. Technol.* **2010**, *101*, 788–793.

(6) Barnoud, F.; Dutton, G. G. S.; Joseleau, J.-P. La D-xylane du roseau *Arundo donax*. *Carbohydr. Res.* **1973**, *27*, 215–223.

(7) Shatalov, A. A.; Pereira, H. Carbohydrate behavior of *Arundo donax* L. in ethanol-alkali medium of variable composition during organosolv delignification. *Carbohydr. Polym.* **2002**, *49*, 331–336.

(8) Coelho, D.; Marques, G.; Gutiérrez, A.; Silvestre, A. J. D.; del Río, J. C. Chemical characterization of the lipophilic fraction of giant reed (*Arundo donax*) fibres used for pulp and paper manufacturing. *Ind. Crop Prod.* **2007**, *26*, 229–236.

(9) Fan, X. F.; Hou, X. C.; Zuo, H. T.; Wu, J. Y.; Duan, L. A. S. Biomass yield and quality of three kinds of bioenergy grasses in Beijing of China. *Sci. Agric. Sinica* **2010**, *43*, 3316–3322.

(10) Ask, M.; Olofsson, K.; Di Felice, T.; Ruohonen, L.; Penttilä, M.; Lidén, G.; Olsson, L. Challenges in enzymatic hydrolysis and fermentation of pretreated *Arundo donax* revealed by a comparison between SHF and SSF. *Process Biochem.* **2012**, *47*, 1452–1459.

(11) Boerjan, W.; Ralph, J.; Baucher, M. Lignin biosynthesis. *Annu. Rev. Plant Biol.* **2003**, *54*, 519–546.

(12) Ralph, J.; Lundquist, K.; Brunow, G.; Lu, F. C.; Kim, H.; Schatz, P. F.; Marita, J. M.; Hatfield, R. D.; Ralph, S. A.; Christensen, J. H.; Boerjan, W. Lignins: natural polymers from oxidative coupling of 4-hydroxyphenylpropanoids. *Phytochem. Rev.* **2004**, *3*, 29–60.

(13) Zhang, X. H.; Chiang, V. L. Molecular cloning of 4-coumarate:coenzyme A ligase in loblolly pine and the roles of this enzyme in the biosynthesis of lignin in compression wood. *Plant Physiol.* **1997**, *113*, 65–74.

(14) Ikeda, T.; Holtman, K.; Kadla, J. F.; Chang, H. M.; Jameel, H. Studies on the effect of ball milling on lignin structure using a modified DFRC method. *J. Agric. Food Chem.* **2002**, *50*, 129–135.

(15) Björkman, A. Isolation of lignin from finely divided wood with neutral solvents. *Nature* **1954**, *174*, 1057–1058.

(16) Lai, Y. Z.; Sarkanen, K. V. Isolation and structural studies. In *Book Lignins: Occurrence, Formation, Structure and Reactions*; Sarkanen, K. V., Ludvig, C. H., Eds.; Wiley-Interscience: New York, 1971; pp 165–240.

(17) Pew, J. C. Properties of powdered wood and isolation of lignin by cellulolytic enzymes. *Tappi J.* **1957**, *40*, 553–558.

(18) Guerra, A.; Filpponen, I.; Lucia, L.; Argyropoulos, D. S. A comparative evaluation of three lignin isolation protocols with different wood species. *J. Agric. Food Chem.* **2006**, *54*, 9696–9705. Wu, S.; Argyropoulos, D. S. An improved method for isolating lignin in high yield and purity. *J. Pulp Paper Sci.* **2003**, *29*, 235–240.

(19) Fasching, M.; Schröder, P.; Wollboldt, R. P.; Weber, H. K.; Sixta, H. A new and facile method for isolation of lignin from wood based on complete wood dissolution. *Holzforschung* **2008**, *62*, 15–23.

(20) Sun, R. C.; Lawther, M.; Banks, W. B. Effects of pretreatment temperature and alkali concentration on the composition of alkali-soluble lignins from wheat straw. *J. Appl. Polym. Sci.* **1996**, *62*, 1473–1481.

- (21) Sette, M.; Wechselberger, R.; Crestini, C. Elucidation of lignin structure by quantitative 2D NMR. *J. Chem. Eur.* **2011**, *17*, 9529–9535.
- (22) del Río, J. C.; Rencoret, J.; Marques, G.; Gutiérrez, A.; Ibarra, D.; Santos, J. I.; Jiménez-Barbero, J.; Zhang, L.; Martínez, A. T. Highly acylated (acetylated and/or *p*-coumaroylated) native lignins from diverse herbaceous plants. *J. Agric. Food Chem.* **2008**, *56*, 9525–9534.
- (23) Lu, F. C.; Ralph, J. DFRC method for lignin analysis. 1. New method for β -aryl ether cleavage: lignin model studies. *J. Agric. Food Chem.* **1997**, *45*, 4655–4660.
- (24) del Río, J. C.; Rencoret, J.; Gutierrez, A.; Nieto, L.; Jimenez-Barbero, J.; Martínez, A. T. Structural characterization of guaiacyl-rich lignins in flax (*Linum usitatissimum*) fibers and shives. *J. Agric. Food Chem.* **2011**, *59*, 11088–11099.
- (25) Sluiter, A.; Hames, B.; Ruiz, R.; Scarlata, C.; Sluiter, J.; Templeton, D.; Crocker, D. *Determination of Structural Carbohydrates and Lignin in Biomass*; Technical Report NREL/TP-510-42618; U.S. GPO: Washington, DC, 2008.
- (26) Asikkala, J.; Tamminen, T.; Argyropoulos, D. S. Accurate and reproducible determination of lignin molar mass by acetobromination. *J. Agric. Food Chem.* **2012**, *60*, 8968–8973.
- (27) Faix, O.; Argyropoulos, D. S.; Robert, D.; Neirincq, V. Determination of hydroxyl groups in lignins evaluation of ^1H -, ^{13}C -, and ^{31}P -NMR, FT-IR, and wet chemical methods. *Holzforschung* **1994**, *48*, 387–394.
- (28) del Río, J. C.; Rencoret, J.; Prinsen, P.; Martínez, A. T.; Ralph, J.; Gutiérrez, A. Structural characterization of wheat straw lignin as revealed by analytical pyrolysis, 2D-NMR, and reductive cleavage methods. *J. Agric. Food Chem.* **2012**, *60*, 5922–5935.
- (29) del Río, J. C.; Prinsen, P.; Rencoret, J.; Nieto, L.; Jiménez-Barbero, J.; Ralph, J.; Martínez, A. T.; Gutiérrez, A. Structural characterization of the lignin in the cortex and pith of elephant grass (*Pennisetum purpureum*) stems. *J. Agric. Food Chem.* **2012**, *60*, 3619–3634.
- (30) Hallac, B. B.; Sannigrahi, P.; Pu, Y.; Ray, M.; Murphy, R. J.; Ragauskas, A. J. Biomass characterization of *Buddleja davidii*: a potential feedstock for biofuel production. *J. Agric. Food Chem.* **2009**, *57*, 1275–1281.
- (31) Yuan, T. Q.; Sun, S. N.; Xu, F.; Sun, R. C. Structural characterization of lignin from triploid of *Populus tomentosa* Carr. *J. Agric. Food Chem.* **2011**, *59*, 6605–6615.
- (32) Buranov, A. U.; Mazza, G. Lignin in straw of herbaceous crops. *Ind. Crop Prod.* **2008**, *28*, 237–259.
- (33) Jääskeläinen, A. S.; Sun, Y.; Argyropoulos, D. S.; Tamminen, T.; Hortling, B. The effect of isolation method on the chemical structure of residual lignin. *Wood Sci. Technol.* **2003**, *37*, 91–102.
- (34) Seca, A. M.; Cavaleiro, J. A.; Domingues, F. M.; Silvestre, A. J.; Evtuguin, D.; Neto, C. P. Structural characterization of the lignin from the nodes and internodes of *Arundo donax* reed. *J. Agric. Food Chem.* **2000**, *48*, 817–824.
- (35) Sun, R. C.; Lu, Q.; Sun, X. F. Physico-chemical and thermal characterization of lignins from *Caligonum monogolicum* and *Tamarix* spp. *Polym. Degrad. Stab.* **2001**, *72*, 229–238.
- (36) Faix, O. Classification of lignins from different botanical origins by FT-IR spectroscopy. *Holzforschung* **1991**, *45*, 21–28.
- (37) Boeriu, C. G.; Bravo, D.; Gosselink, R. J. A.; Dam, J. Characterisation of structure-dependent functional properties of lignin with infrared spectroscopy. *Ind. Crop Prod.* **2004**, *20*, 205–218.
- (38) Jiao, J. J.; Zhang, Y.; Liu, C. M.; Liu, J. E.; Wu, X. Q.; Zhang, Y. Separation and purification of tricrin from an antioxidant product derived from bamboo leaves. *J. Agric. Food Chem.* **2007**, *55*, 10086–10092.
- (39) Wen, J. L.; Sun, S. L.; Xue, B. L.; Sun, R. C. Quantitative structural characterization of the lignins from the stem and pith of bamboo (*Phyllostachys pubescens*). *Holzforschung* **2013**, DOI: 10.1515/hf-2012-0162.
- (40) Crestini, C.; Argyropoulos, D. S. Structural analysis of wheat straw lignin by quantitative ^{31}P and 2D NMR spectroscopy. The occurrence of ester bonds and α -O-4 substructures. *J. Agric. Food Chem.* **1997**, *45*, 1212–1219.
- (41) Martínez, A. T.; Rencoret, J.; Marques, G.; Gutiérrez, A.; Ibarra, D.; Jiménez-Barbero, J.; del Río, J. C. Monolignol acylation and lignin structure in some nonwoody plants: a 2D NMR study. *Phytochemistry* **2008**, *69*, 2831–2843.
- (42) Kim, H.; Ralph, J. Solution-state 2D NMR of ball-milled plant cell wall gels in DMSO- d_6 /pyridine- d_5 . *Org. Biomol. Chem.* **2010**, *8*, 576–591.
- (43) del Río, J. C.; Rencoret, J.; Marques, G.; Li, J. B.; Gellerstedt, G.; Jimenez-Barbero, J.; Martínez, A. T.; Gutierrez, A. Structural characterization of the lignin from jute (*Corchorus capsularis*) fibers. *J. Agric. Food Chem.* **2009**, *57*, 10271–10281.
- (44) Lu, F. C.; Ralph, J. Novel tetrahydrofuran structures derived from β - β -coupling reactions involving sinapyl acetates in kenaf lignins. *Org. Biomol. Chem.* **2008**, *6*, 3681–3694. Lu, F. C.; Ralph, J.; Novel β - β structures in lignins in incorporating acylated monolignols. *Appita J.* **2005**, 223–237.
- (45) Kuwabara, H.; Mouri, K.; Otsuka, H.; Kasai, R.; Yamasaki, K. Tricin from a *Malagasy connaraceous* plant with potent antihistaminic activity. *J. Nat. Prod.* **2003**, *66*, 1273–1275.
- (46) Ralph, J.; Landucci, L. L. NMR of lignins. In *Lignin and Lignans; Advances in Chemistry*; Heitner, C., Dimmel, D. R., Schmidt, J. A., Eds.; CRC Press (Taylor & Francis Group): Boca Raton, FL, 2010; pp 137–234.
- (47) Lu, F. C.; Ralph, J. Detection and determination of *p*-coumaroylated units in lignins. *J. Agric. Food Chem.* **1999**, *47*, 1988–1992.
- (48) Akiyama, T.; Matsumoto, Y.; Okuyama, T.; Meshitsuka, G. Ratio of *erythro* and *threo* form of β -O-4 structure in tension wood lignin. *Phytochemistry* **2003**, *64*, 1157–1162.
- (49) Lu, F. C.; Ralph, J. The DFRC method for lignin analysis. 2. Monomers from isolated lignins. *J. Agric. Food Chem.* **1998**, *46*, 547–552.